Deep Convolutional Residual Regressive Neural Networks and Sea Surface Temperatures from Aqua & Argo in the 2000s

Abstract

Sea surface temperature (SST) is an essential climate variable that can be measured via ground truth, remote sensing, or hybrid model methodologies. Here, we celebrate the progress of high resolution sea surface temperature via the technological advances of the late 20th and early 21st century. Specifically, we observe three snapshots of twelve monthly SST measurements in 2010 as measured by the passive microwave radiometer AMSR-E, the visible and infrared monitoring MODIS, and the in situ Argo dataset ISAS produced by the Laboratoire d'Océanographie Physique et Spatiale. We author some simple scripts to perform the functions of an extract, transform, and load (ETL) system. We furthermore pay homage to the early 21st century advances in artificial intelligence: specifically, we experiment with a machine learning technology known as deep convolutional residual regress neural networks and attempt to fuse AMSR-E and MODIS into a superior product. We have mixed results: on the one hand, we have constructed a flexible grassroots approach to extract, transform, load, and data assimilation called Flux to Flow (F2F); on the other hand, data assimilation here appears limited by coastal land sea interface artifact. Looking forward, we hope to integrate F2F with future satellite missions such as Surface Water Ocean Topography (SWOT) or Interferometric Synthetic Aperture Radar (InSAR) to enhance the precision of coastal regions observations of water.

1. Intro

Under the auspices of its 193 member states, the World Meteorological Organization holds of particular importance certain physical measurements of Earth and the surrounding environment. Each parameter is singled out by being promoted under the acronym **ECV**, denoting the physical measurement to be an **E**ssential **C**limate **V**ariable. Furthermore, the same organization has established goals and deadlines for the participating countries to sustain all forms of life on earth, known as sustainable development goals or **SDG**s.

Evidence continues to mount that human beings through industrialization have modified and are continuing to significantly modify the climate. However, the modern cause for concern is the rate at which our climate has changed rather than the binary question of (has it / has it not). Measurements of CO_2 tell the story: detected values of atmospheric CO_2 have increased by 50% of the starting value at the advent of industrialization (NASA, 2022). Invariant to latitude and longitude, the impacts are felt everywhere. Earth's response to our stimuli manifests in the form of heat waves, stronger storms, longer periods of drought, greater impulses of meteorological water accumulation over land, and a general increase in environmental variability. While in wealthy communities, modern civil infrastructure serves as a boundary layer to environment-related catastrophes, the poor and powerless are unequally yoked. One must consider also the importance of the ecology itself. As humanity conquers the environment, in what state are the creatures of the atmosphere, land and oceans? What does the next five, ten, five hundred years look like at the current rate? If deemed unacceptable, what changes can be made to mitigate or adapt to implications of past and present poor actions? What are the global environmental quality standards? How can standards be enforced in unequal nation states?

There are many global environmental observation systems that study the entire Earth from a distance. The sheer volume of effort and observation output can be gleaned by world wide web crawling one example: the details of the Coupled Model Intercomparison Project website. Through this project, expert parties from all over the globe share the effort of simulating Earth by focusing on their separate silos whilst having common tunnels to assemble, communicate, benchmark, and improve. Remote sensing (RS) instruments have recently (1950 – present) grown in frequency of occurrence, capability, availability, and affordability. Attached to planes, balloons, spacecraft, or other autonomous means, these devices capture images in a controlled fashion over medium to large portions (swaths) of the land, atmosphere, and ocean. The growth of global RS data is pivotal to our ability to continuously view the macroscopic climate system. The output of these RS devices can be studied with a variety of optical techniques, in most cases altered via some logic to provide a more value-added product depending on the data consumer's needs. For example, consider the delineation of processing levels provided in the peer-reviewed document coinciding with the deployment of the ECOSTRESS instrument (Fisher et al, 2019). A lower value processing level (L0, L1) indicates a raw measurement of electromagnetic radiation from the Sun through Earth's atmosphere off the land / water surface, back up to through the atmosphere to the satellite instrument. In turn, a higher value (L2 – L4) indicates the generation of physical parameters, gridding of swath data, and data assimilation with other parameters. In the instance of ECOSTRESS, the higher levels refer to land surface temperature/emissivity, measures of evapotranspiration, and at Level 4 evaporative stress and water use indices.

Here, we investigate the ocean's surface temperature (SST). This target is chosen because of its focus on the behavior of water in the environment, its importance in numerical weather / climate forecasting and its detectability via satellite-mounted RS instrumentation. Also, it has matched continuous ground truth (in situ) temporospatial twin measurements that can be investigated for intercomparison of dataset bias / variances / uncertainties. While it is not practical to grid the entire surface of Earth with sensors, in many situations and places it is extremely valuable to use arrays of dense, spatially linked precise in situ measurements. Satellite observations have a coarse resolution and are known to miss sub-mesoscale and even simply mesoscale anomalies within the hydrosphere (atmosphere, land, ocean).

We compare the raw satellite observations to the lower resolution but more precise (less susceptible to high noise) measurements of sea surface temperature. We apply a treatment to the lower resolution but generally more available satellite instrument (AMSR-E), setting its target output to be the higher resolution MODIS product. Our hypothesis is that fusing the AMSR-E data to MODIS data will create a product that is closer in performance to MODIS than its AMSR-E input. While we have global availability of data in the monthly product that combines many swaths of Aqua observations, the Level 2 MODIS product suffers from severe cloud contamination. The combination of wide radiometer coverage and high infrared resolution might be successfully combined to form a superior product in near real-time following data acquisition such as that obtained by AMSR2, VIIRS, or another future mission. We also see future uses of this treatment in forecasting more accurate river streamflow based on RS data. The architecture could also be adapted as a control mechanism on future missions. An anomaly detection system onboard a cluster of CubeSats that relays when information is significantly abnormal in a

location relative to its usual behavior might help maximize the productivity of articulating environmental monitoring systems on places of interest based on a learned representation.

2. Materials / Methods

Sea Surface Temperature (SST)

Sea surface temperature (SST) as a continuously monitored variable started when Benjamin Franklin captured measurements of the ocean as he traversed the Atlantic, acquiring data and synthesizing these observations into information about the Gulf Stream. There is a rich history from that point forward to the present day, with a thorough review available in the literature (Minnett et al, 2019).

Though SST is largely academically segregated in the field of physical oceanography, the connection between ocean, atmosphere, and land are evident in the climatological visualizations of SST upon the rest of the hydrosphere. There is a trickling down from global SST to the availability of food, energy, and clean drinking water. Consequently, better understanding and application of oceanic parameters in consideration of land-based hydrology opens the door for improved forecasting and preparation for the future.

Aqua

The Aqua satellite was launched on May 4, 2002. Upon it, two instruments sit: AMSR-E and MODIS. Both, among other things, are designed to study the temperature of the ocean. The measurements obtained as the satellite is moving from South Pole towards North always crosses

the equator at approximately 1:30 PM local time nadir (directly below the satellite). In the downward portion of the orbit, the satellite crosses the equator at 1:30 AM local time nadir.

AMSR-E

AMSR-E is a passive microwave radiometer. The acronym stands for Advanced Microwave Scanning Radiometer for Earth Observing System. There are several products produced on top of the raw radiance data collected by this instrument. The AMSR-E data is processed by different locations depending on the parameter of interest. The produced datasets contain latitude, longitude, several physical parameters (e.g., SST, Albedo, soil moisture) as well as other pertinent metadata. As it pertains to sea surface temperature, AMSR-E is available in Level 2 or Level 3 products and as part of Level 4 assimilation system output.

AMSR-E Level 2 and 3 Data Variables		
File Name	Unit	Description
sea_surface_temperature	K	Subskin temperature
sst_dtime	s	Time Difference from Reference Time
dt_analysis	s	Deviation from SST Reference Climatology
sses_bias	K	Single Sensor Error Statistic Bias
sses_standard_deviation	K	Single Sensor Error Statistic Standard Deviation
l2p_flags		Fifteen unique pixel classifications
quality_level		0-5 scale, 0–-no data, 1–bad data, 5–best quality
wind_speed	m s-1	Wind Speed
diurnal_amplitude	K	Estimated Diurnal Variability
cool_skin	K	Cool Skin Factor
water_vapor	kg m-2	Columnar Mass Concentration of Water Vapor
cloud_liquid_water	kg m-2	Cloud Liquid Water
rain_rate	mm hr-1	Rainfall Rate
sea_ice_fraction	/1	Sea Ice Fraction

rejection_flag		Only included in Level 3, redundance to quality_level and l2p_flags
confidence_flag		
proximity_confidence		

To detail a sample, one single Level 2 netCDF (.nc) file was downloaded and opened through the Remote Sensing System's OPeNDAP data system. The record selected is that of March 3rd, 2004, with a UTC time of 01:07:01. The file contains three coordinates (latitude, longitude, and time) and thirteen data variables reproduced from the .nc in Table 1.

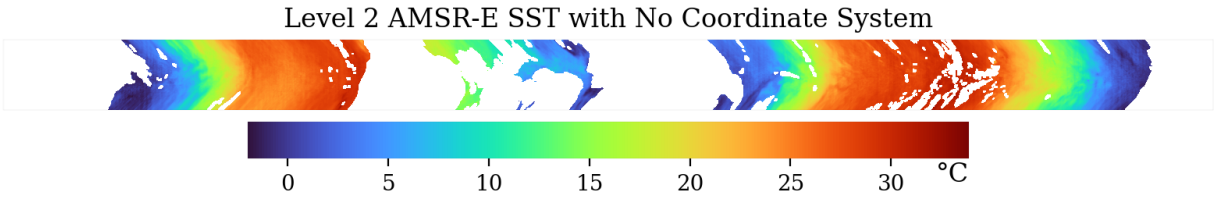

Figure 1

Each variable is a single matrix comprised of columns and rows of measurements. The important distinction here is that the data structure is stored to reflect the path of the orbit. See Figure 1. When the sea surface temperature is plotted as it sits in the matrix, it is difficult to discern what is transpiring. There appears to be some curvature of the measurements, but other than that little is known to an untrained eye beyond the title and colormap.

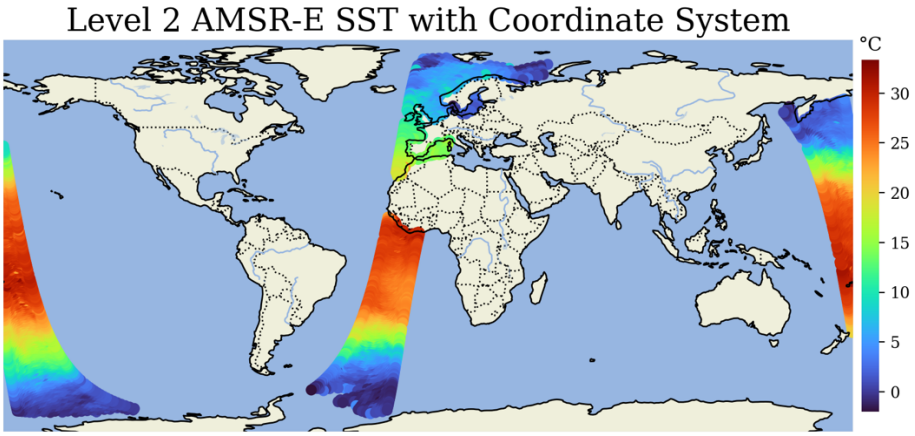

Figure 2

Inclusion of the latitude and longitude coordinates, as well as a geographic information system generates a clearer picture as seen in Figure 2. A single Level 2 AMSR-E SST file contains matrices representing one full orbit around the globe. Each file contains partially daytime and partially nighttime observations. Because of diurnal warming, it is desirable to separate the nighttime and daytime passes. Furthermore, many analyses are comprised of an ensemble of satellite observations from different platforms such as this one. It is relatively inconvenient to numerically and spatially analyze multiple swath-based Level 2 observations concurrent with an in situ target. A grid makes for more orderly computations at large spatial scales. Certainly, one could elect to grid every observation to the AMSR-E or MODIS native product coordinate system. Here, we use Level 3 because of the interest in spatial relationship across large geographic scales and variable time (daily, weekly, seasonally, yearly, generationally).

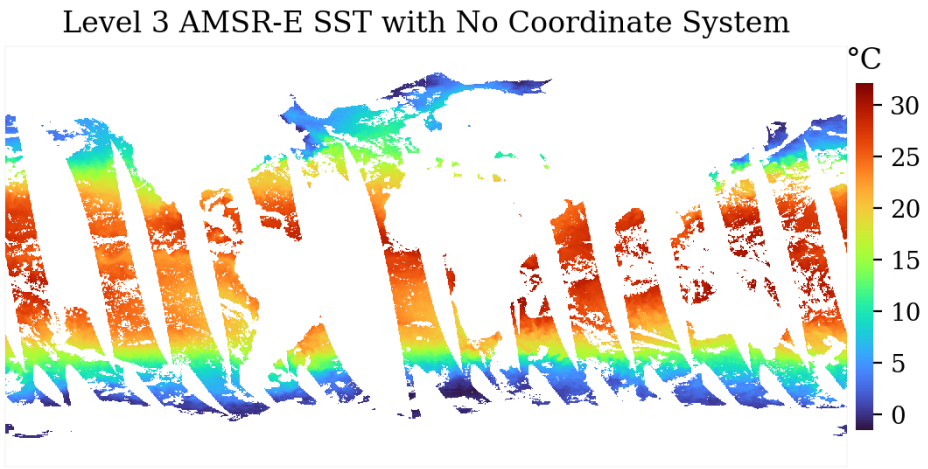

Figure 3

The Level 3 equidistant rectangular gridded product (AMSRE-REMSS-L3U-v7a) is accessed via the NASA Jet Propulsion Laboratory's Physical Oceanography Distributed Active Archive Center (PODAAC) and was produced by Remote Sensing Systems (Santa Rosa, CA). This product comes in 25km resolution and is delineated by daytime and nighttime passes of the satellite. The time series runs from June of 2002 until October of 2011 when the AMSR-E instrument ceased functioning. Figure 3 illustrates the point that even without explicitly defining the coordinate system in the visualization, the matrix of SST values is already placed in proper spatial order. Figure 4 reinforces the fact that little change occurs with the inclusion of latitude and longitude coordinates when plotted on a rectangular grid.

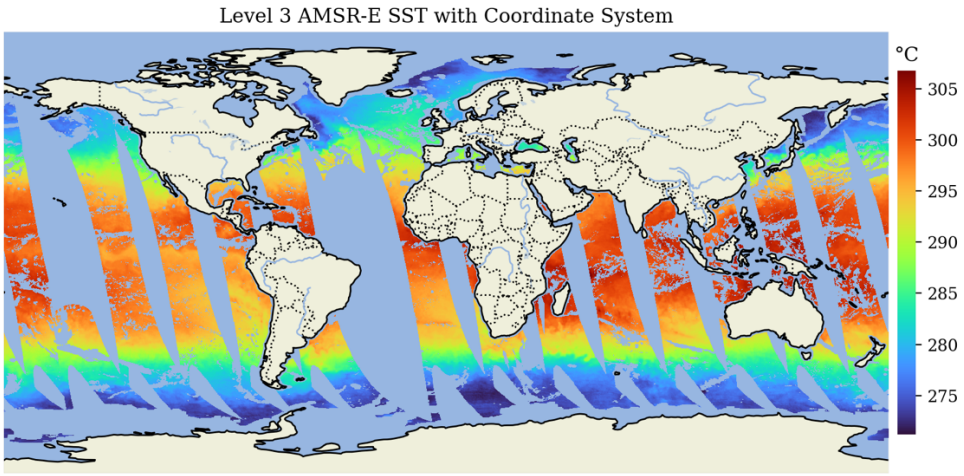

Figure 4

We accumulate the daily daytime and nighttime readings from AMSR-E into monthly products. While a monthly product has already been produced for use with the Climate Model Intercomparison Project, AMSR-E_CMIP5 as available from the PODAAC as of this writing does not delineate between daytime and nighttime. Here, we simply compute the monthly average for daytime and nighttime passes on a pixel-wise basis for each month. We finally re-grid the AMSR-E data to the MODIS coordinate system.

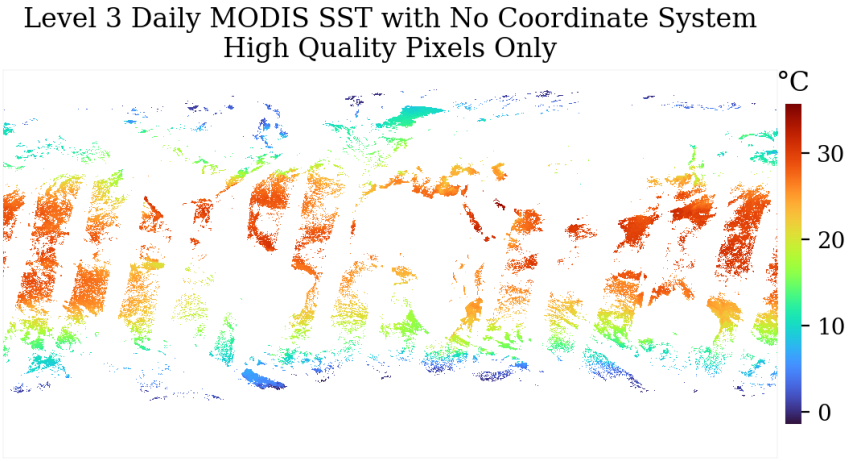

Figure 5

MODIS

MODIS, or Moderate Resolution Imaging Spectroradiometer, measures thirty-six different radiance bands in the infrared and visible ranges of the electromagnetic spectrum. Level 3 sea surface skin temperature as obtained from MODIS comes in 4km and 9km products and is derived from a subset of the thirty-six radiance bands. The products are available in daily, average of eight days, and monthly products. They are also delineated by daytime and nighttime passes of the Aqua's polar-orbiting nature. SST products deriving from MODIS are further specified by the length of the waves within the thermal infrared range used to derive the measurement: longer waves (11–12 microns) and middling waves (3–4 microns). The MODIS documentation state that the 3–4 micron wave SST product is less uncertain, but only usable at night because of the daytime sun glint impact on 3–4 micron waves. We use the long wave 11–12 micron infrared measurements to keep constant the source of both daytime and nighttime passes.

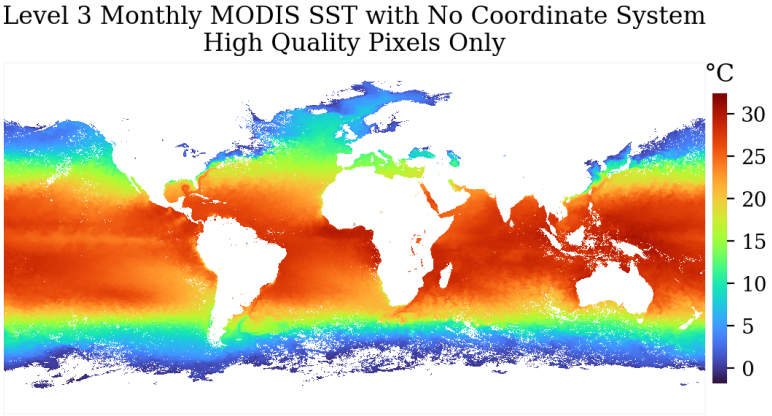

Figure 6

The MODIS Aqua Level 3 SST Thermal IR Monthly 4km V2019.0 product comes with latitude and longitude coordinates, SST values and per pixel quality measurements denoting when

contamination is likely. The grid is equidistant rectangular, a match with the AMSR-E grid but at a finer original resolution. Of the over 30M pixels for an entire day of 4km MODIS pixels, 90% of them in the random sample selected here are deemed contaminated and filtered out (Figure 5). This contrasts with the 50% loss of AMSR-E pixels. This great loss in pixels due to quality is attributed to cloud contamination. To compensate, we use the monthly product (Figure 6) where a greater amount of time has transpired, allowing for a higher probability of clean global coverage. A randomly sampled MODIS monthly image yields 50% loss, in line with the AMSR-E daily product and much improved upon relative to the daily MODIS observation files.

MODIS Level 2 and 3 Data Variables https://podaac-tools.jpl.nasa.gov/drive/files/allData/modis/L3/docs/modis_SST.html		
File Name	Unit	Description
SST	deg C	Skin temperature
qual_SST		0 = good, 1 = questionable, 2 = clouds, 255 = land, gross clouds, other errors. 0 is recommended.

Table 2

In situ measurement system

We selected the "In Situ Analysis System" (ISAS) dataset obtained from the University of California's Argo repository and produced by a consortium of French institutions (Gaillard et al., 2016). An important constraint is the desire to obtain *only* the surface level measurement of temperature at the highest global frequency available during the operating years of both AMSR-E and MODIS. These products are provided in a gridded format are used to observe temperature measurements at many depth levels. In the publication attached to the dataset, the target physical quantity is steric height and ocean heat content; with these as their target output, gridded depth-

dependent temperature is stored as a byproduct. The 0.5 degree monthly dataset is presented in a Mercator projection, slightly different than the AMSR-E and MODIS grids. Mercator lines of longitude have a uniform distance in between them; the distance between latitudes from the equator changes. Identical to AMSR-E, we re-grid this data to the MODIS grid and coordinate system.

Treatment

The treatments we apply to the data are several configurations of one common concept: neural networks. Neural networks are not new, but the growth of graphical processing units (hardware) has enabled them to flourish in software. Neural networks are a type of learned representation. A structure is fed connected input and target pairs. Based on the predictive quality of the initial network structure, an error between the neural network output and the target occurs. This error is in turn fed to a linear optimization algorithm that iteratively and slightly alters each "neuron" of the initial network structure until it reaches a designated optimal state. Via many small calculations and the simultaneous application of statistical mechanics, neural networks are known to provide qualities like that of a brain, such as capturing spatial eccentricities and temporal changes in sets of related images. Neural networks are applied to a range of tasks from the more mundane such as learning a quadratic equation, to the more cutting edge, like extreme event forecasting or cancer detection.

Transfer learning has become commonplace, placing an emphasis in academic research to not just have the best results, but to provide the treatment structure for others to build on top of without inadvertently causing the audience to get lost in the details. To a degree, we employ

transfer learning to relatively easily create a complex configuration. The neural network is characteristically deep, convolutional, residual, and regressive. Our construct is inspired by the work documented in He et al., 2016. However, our problem is one of a regressive nature. Sea surface temperature has a limited temperature range that it exists within. This is a notable difference to some of the more common introductory neural network examples, such as those associated with the MNIST and CIFAR datasets. Regressive loss functions are constrained to just a couple: mean absolute error (MAE) and mean squared error (MSE). The calculation of the loss function must be differentiable. This constraint is due to the optimization component of neural networks. The reader is redirected to output like that in Andrychowicz et al., 2016 or Kingma and Ba, 2017 for further reading of neural network optimizer mechanics.

Once the network architecture and all hyperparameters are chosen, training and validation data is loaded into the network. While training the neural network, close observation is made of the reduction in error between training input and output as the neural network begins to learn the representation. We also monitor the validation dataset at each training iteration. The learning process stops once the training data passed through the optimized network achieves a relative minimum according to the loss function (MAE or MSE) between training model output and target. At this point, the optimized neural network structure is intentionally frozen. Before freezing, the many neurons of the network can be adjusted to optimize, like asking a teacher for advice when studying. The frozen state and inference imposed upon it is like a student being prompted with a test of new problems and no teacher assistance. This test or input data are similar enough to the training for success in passing the test according to the selected merit.

A learned representation *can* become biased to its training inputs. It starts to memorize the training dataset, which does not make for a generally applicable algorithm. Avoidance of biasing comes at the cost of variance (Geman et al., 1992). Applying dropout is one technique to systematically prevent system bias by simply "turning off" a certain percentage of random neurons at each iteration of the algorithm (Hinton et al., 2012; Srivastava et al., 2014). Another approach is the application of early stopping. The loss function of a neural network typically looks like a very steep curve down to a flat bottom. Rather than allow the network to persist in the flat bottom for long and become overfit, simple logic can be employed to stop training early when the network shows evidence that it has reached an optimal state. Percentage of data split between training, testing, and validation proportions is another relevant training hyperparameter. A larger proportion of the dataset being part of the training portion could lead to overfitting of the model and lack of generalized predictability. On the other hand, insufficient training data might lead to an inability to adequately characterize the reality of the data pairs. We have made the code and examples are available here.

The image sets subjected to treatment are on the large side computationally. Holding many 1M or 9M pixel images within the memory of a single graphical processing unit becomes intolerable to the device. One could elect to use multiple GPUs or a compute node with a great provision of memory. Here, we constrain the experiment to a single GPU and cut the images up into smaller pieces of square data. Our patch size is fixed at 100 x 100, though this is a tunable hyperparameter. Figure 7 shows a Pacific Ocean study region, highlighting Hawaii and regions east. While this image is too large to process directly in the neural network, we can solve this

problem by creating the eighteen patches of 100 x 100 pixels, representing the 300 x 600 pixel region under observation.

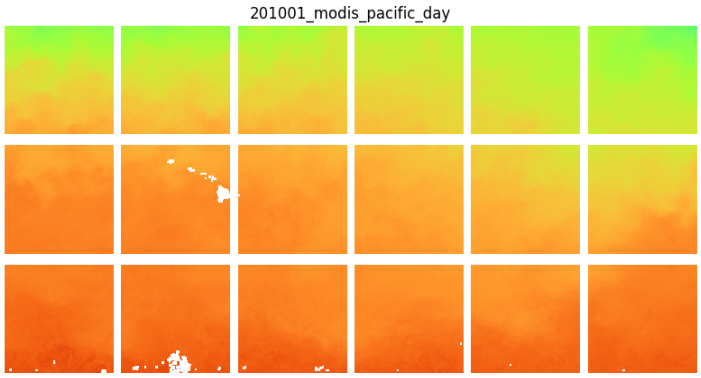

Figure 7: Sample training monthly observation, here January 2010 MODIS day looking at Hawaiian Islands and segmented into 100 x 100 pixel regions.

Neural networks do not function when ‘nan’ values are present in any of the images. We enacted a broad treatment to the AMSR-E and MODIS images, computing the mean of the entire 1M or 9M pixel image, excluding the nan values. Then, where the nan values are present, we replace them with the mean value. This has the convenient byproduct of introducing into the neural network many training pairs where the input and output are simply comprised of the average global SST value as obtained via the AMSR-E and MODIS instrument. As there is the potential for systemic bias due to the nature of the phenomenon known as sea surface skinning which appears predominantly in times of low winds (Figure 8), we hypothesize that the neural network processing of many similar observations comprised of predominantly averages of the two datasets serves as a potential native bias correction filter.

Beyond nan-filling, we also whiten the values around their 100 x 100 pixel neighbors. Whitening the data is shown to improve the computational speed. We retain the mean and standard

deviation of certain patches so the whitened patches can be inverted back into SST for human analysis and intercomparison among the panel of SST fields post treatment. For our optimally interpolated 4km product, in the post treatment stage we apply the MODIS land water mask product obtained through NASA's Land Processes Distributed Active Archive Center, and filter highly irregular measurements seen along the coastlines.

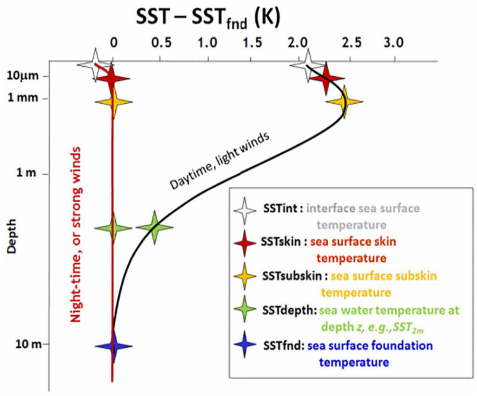

Figure 8: Sea surface skin effect from (Minnett et al, 2019)

Results

We prepared the data for nine different cases all studying the year 2010: the **A**tlantic, **P**acific, and **I**ndian Oceans segmented by monthly **D**ay, **N**ight, and **H**ybrid (day and night averaged) observations of SST. We train the neural network on the first ten months of the year, validate with the eleventh month, and test with the twelfth month. Each training session runs for 100 epochs or forwards backwards propagations through the entire training dataset. Each image in the geographically constrained time series is 300 pixels x 600 pixels in size, divided up into eighteen 100 x 100 pixel segments to incrementally feed the neural net.

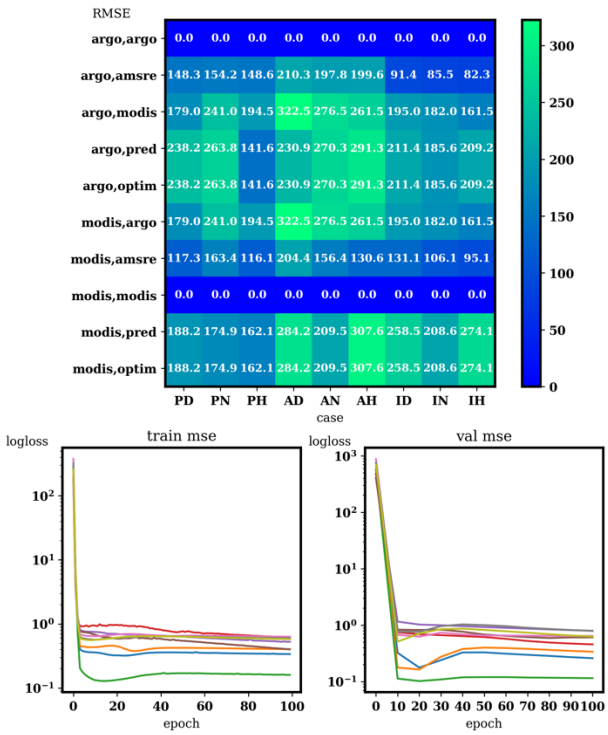

Figure 9: Aggregate results of the nine SST case studies

In all instances, both training and validation loss functions drop by several orders, indicating successful training without overparameterization as would be indicated by low training error but high validation error. Performance of network as it relates to the test data, December 2010, is

seen in the upper plot of Figure 9. The goal is for measurements involving ‘pred’ or ‘optim’ to bring the RMSE value between AMSR-E and Argo or MODIS down. The optim case has superior coverage because it gapfills any spaces where there is a valid measurement in exactly one of two datasets, the model prediction from AMSR-E input through the neural network or the MODIS target. However, in some instances what it fills with doesn’t appear much better than filling with a nan value instead.

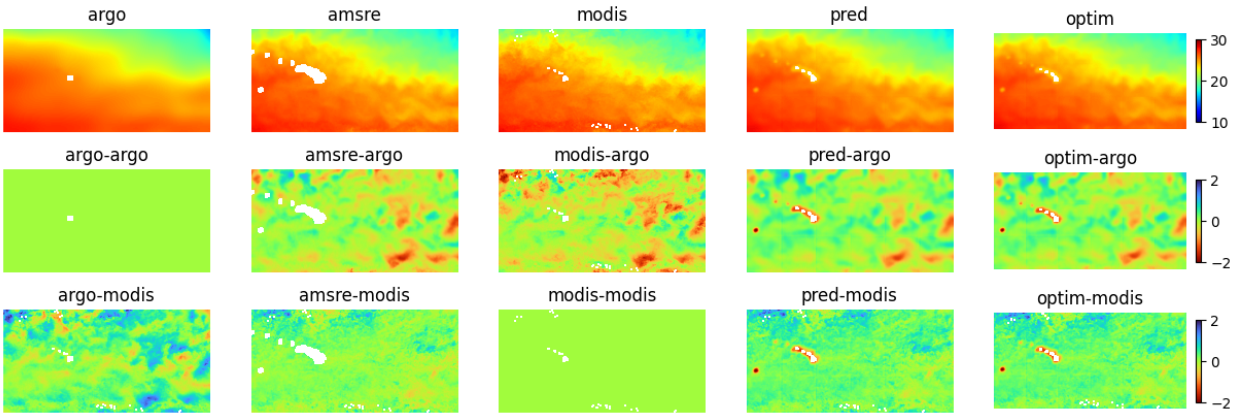

Figure 10: Relatively “good” perceptual change, Pacific Night case

In every case, the RMSE between the optim and MODIS is higher than the AMSR-E input. In some instances, the test case of December does make an optim output that is closer to Argo than the input AMSR-E. In some cases, though, it makes a worse performing product with regards to Argo than either AMSR-E or MODIS. A bright spot is that the optim output is closer to MODIS than the Argo product. See Figures 10 and 11 for samples of how the RMSE translates to actual transformation of the images.

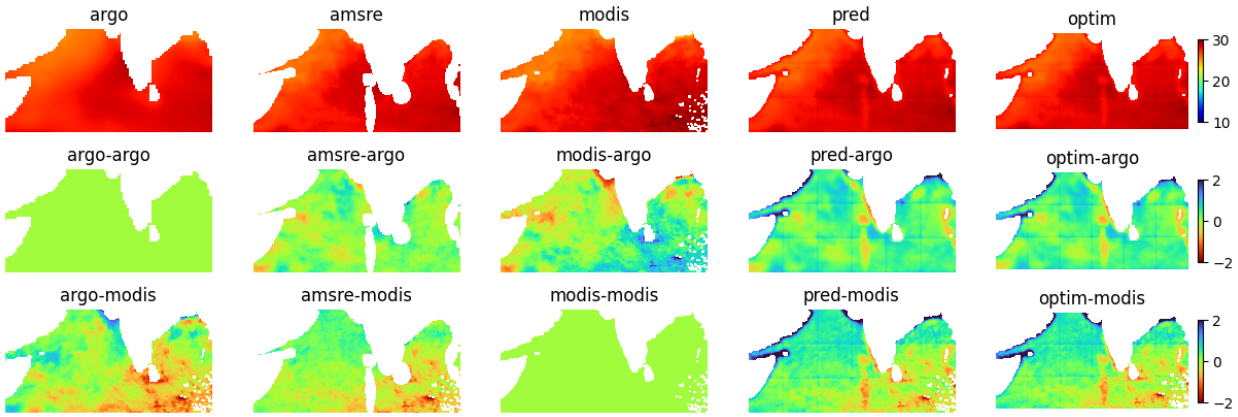

Figure 11: Relatively “poor” perceptual change, Indian Day case

Discussion

Within the constraints of this experiment, while the continual development of a relatively open, hybrid RS-ETL (extract, transform, load) (Bansal and Kagemann, 2015) system along with creation of the actual destination for the RS-ETL (namely the neural network treatment and posttest analytics) is certainly a plus, the results of this study request future engagement. In every case of this study, the neural network appears to struggle with coastal regions. This is due to the nature of the land sea boundary layer in all these datasets. It is what might be commonly addressed by computer scientists as an ‘edge case.’ At the presence of land, the pixel is plotted as white and is given a not-a-number (nan) designation. Neural networks weren’t really designed for the currently produced segregated RS datasets. The datasets appear to be manufactured with the understanding that one group of people are still more interested in ocean behaviors, another land behavior. For the purpose of training a neural network using the convolutional flavor, images with no nans are needed. As referenced earlier, steps were taken during the training process to circumvent the presence of land by substituting those pixels temporarily with the local mean value. Another option is the application of the substitution of the nan values with the mean

as computed by the entire “scene” or day. To be frank, these are more workarounds than true solutions to the image processing problem. There is the potential and a likelihood that the substitution of these values is introducing a source of structured noise. This structured noise likely causes higher than preferable results as denoted in Figure 9. Furthermore, it is probable that this structured noise is hindering training of the neural network process itself.

As it relates to computer vision tasks such as this set of experiments, the use of mean squared error as a loss function has been called into question as an appropriate target (Wang and Bovik, 2009). Their results certainly warrant some concern, and our experiments have some corroboration with their findings. Our images are single channel inputs and can be considered grayscale pictures. When displaying SST images, we use a colormap based on what we know to be the physical limits of the parameter itself. This is a different approach than typical of image based machine learning techniques. Alternate loss functions to the standards baked into PyTorch are available (Kastryulin et al., 2022). These functions innately want the inputs to be either between 0 and 1 (grayscale) or 0 and 255 (color images). We can certainly convert our images to one of these scales and use a z-scoring technique (Larson, 2023). Focus on remote sensing imagery specific loss functions is less common territory. The use of advection and diffusion is one promising avenue (de Bézenac et al., 2019). While neural networks are a useful tool, they alone are not a silver bullet, especially as it relates to geophysics. However, the neural network community has a keen interest in computational efficiency. Practitioners of other machine learning methodologies should take heed as it relates to model training run times, file sizes, ease of transferring the technologies to others.

We applied a land mask generated from the MODIS instrument. Aqua has far surpassed its projected useful life span and was designed before the new millennium. The new Surface Water Ocean Topography (SWOT) mission was only recently launched as of the writing of this document. Datasets from this mission aren't due to be available until late 2023. It will hopefully bring many new insights to the larger water science community. Among those insights are a more precise global picture of Earth's coastal regions. Our hope is that this moment will be one where the authors of these and adjacent water datasets might consider the reduction of nan values by assimilation of land and sea measurements into one cohesive mass.

We only observed a fraction of the available data. The ISAS Argo dataset was a single file attached to a DOI address. We extracted simple the surface layer of this dataset. There is value in consideration of SST depth layers. Furthermore, we studied monthly time series images of all three raw datasets. AMSR-E and MODIS each have near complete global pictures within two to three days (revisit time). These datasets are then transformed in different ways and can lose fidelity by various types of decimation such as regridding from swaths to squares (Zhuang, 2022), uncertainty in formulas used for conversion from base input to high level [L2, L3, L4] physical parameter, or compression. Though out of scope here, it is worthwhile to consider the formation of the inputs used for the study here. Additionally, cloud cover is a persistent factor at play within the community. The question of "is the measurement (pixel) currently observed impacted in an undetectable way?" can't fully go away, because even at the hyperlocal "nowcasting" time scale there is missed detection of events. Because of the pervasive challenges, people need to come together. Great global solutions require more cooperation, engagement, and the act of building bridges with one another. Missions like the International Space Station,

Artemis, Landsat, and GRACE, and SWOT are only examples of what global cooperation can result in. Here at the microscopic level of single parameter consideration, we need more of the same type of teamwork. Dynamic collaboration amongst many stakeholders raises the economic efficiencies of all. Improvement of just a single ECV requires takes the participation of a deep supply chain. Though logistically complex, it's necessary. Water is life and connects the global ecosystem in every facet of life, from food supplies, health of exotic wild animals, to the manufacturing of semiconductor chips and the treatment of industrial water. A clearer perspective is always welcomed to help sustain life. The missions of Aqua and Argo certainly achieved their planned missions in that regard.

Conclusion

Sea surface temperature is an essential climate variable and crucial for the movement of water throughout the hydrosphere. The beginning of the 21st century marked a new frontier in the measurement of SST via the Aqua mission and Argo program. Here, we observe three overlapping datasets focused on measurements of sea surface temperature: AMSR-E microwave measurements, MODIS infrared measurements, and ISAS Argo float ground truth measurements. We focus the study on three large oceanic regions: Indian, Pacific, and Atlantic. We apply Flux to Flow, an extract, transform, and load (ETL) framework combined with a neural network treatment system post-processing analytics test stand. We attempt to transform the coarser resolution satellite product towards the finer one and intercompare all datasets. While the neural network performs well according to its typical loss functions, we find that the presence of frequent 'nan' and the limitations of MSE as a loss function used in computer vision tasks results in limited success when applying the neural network transformation. However, the

techniques here are certainly valuable when taking a grassroots approach to data assimilation. Some would rather homebrew their own combination of low level datasets rather than simply adhere to the provided higher level offerings.

We see the future of this framework including other treatment algorithms such as XGBoost, Transformers, Bayesian Neural Networks, Graph Neural Networks, random forests. We also see a future where fewer output target values are considered (<10 streamflow pixels per output as opposed to the 10,000 pixel image size used here). On the grander scale, the framework could be used as an RS based anomaly detection system (Růžička et al., 2022).

Code Availability

Scripts are available at https://github.com/albertlarson/aqua